Modelling CO 2 transfer in foil ripened semi-hard Swiss-type cheese

F. Acerbi, Valérie V. Guillard, M. Saubanère, C. Guillaume, Nathalie Gontard

Accepted Manuscript

Modelling CO_2 transfer in foil ripened semi-hard Swiss-type cheese

F. Acerbi, V. Guillard, M. Saubanere, C. Guillaume, N. Gontard

PII: S0260-8774(17)30458-2

DOI: 10.1016/j.jfoodeng.2017.10.025

Reference: JFOE 9058

To appear in: *Journal of Food Engineering*

Received Date: 30 May 2017

Revised Date: 27 October 2017

Accepted Date: 28 October 2017

Please cite this article as: Acerbi, F., Guillard, V., Saubanere, M., Guillaume, C., Gontard, N., Modelling CO_2 transfer in foil ripened semi-hard Swiss-type cheese, *Journal of Food Engineering* (2017), doi: 10.1016/j.jfoodeng.2017.10.025.

Journal of Food Engineering

1 ~~**Modelling CO_2 transfer in foil ripened cheese with CO_2 production**~~

2 # Modelling CO_2 transfer in foil ripened semi-hard Swiss-type cheese

3

4 F. Acerbi[a], V. Guillard[a*], M. Saubanere[b], C. Guillaume[a], N. Gontard[a]

5 [a]UMR 1208 IATE Agro-polymer Engineering and Emerging Technologies, Montpellier (France),

6 University of Montpellier, INRA - 2 place Viala - bât. 31, F-34060 Montpellier Cedex 01

7 [b]UMR 5253 - Institut Charles Gerhardt, Montpellier (France), Place Eugène Bataillon, 34090 Montpellier

8 * corresponding author: valerie.guillard@umontpellier.fr

9

Abstract

~~Eye growth in cheese with intense CO_2 production during ripening mainly depends on CO_2 production and transfer properties.~~ Despite CO_2 production and diffusion during ripening of semi-hard Swiss-type cheese ~~eyes in such cheeses~~ are considered as important quality parameters, the research concerning key gas production and transfer in cheese remains widely overlooked. In this study, experimentally assessed CO_2 production was coupled with transfer coefficients in a mathematical model in order to predict CO_2 gradients formed inside the cheese during ripening. The permeability coefficient of CO_2 through the multilayer barrier packaging which wraps the cheese during ripening was also included in the model. The presented model was validated by assessing the CO_2 concentration in the cheese and its partial pressure in the packaging headspace. CO_2 production rate was found to be the most important input parameter affecting CO_2 gradients formed in cheese during ripening whereas the other input parameters (solubility, diffusivity, permeability) had little effect on the total CO_2 gradient.

Keywords: solubility, diffusivity, permeability, CO_2, cheese ripening

25

Nomenclature

α	Level of statistical significance
A	Surface (m^2)
Bi	Biot number (non-dimensional)
br	Bottom rind position of the cheese
C	Concentration (kg/m^3)
ch	Relative to cheese
D	Effective diffusivity coefficient of CO_2 in cheese ($m^2\ s^{-1}$)
exp	Experimental values
HS	Packaging headspace
I	Relative to the interface
j	Relative to a gas specie
k	External mass transfer coefficient (m/s)
K	Degree in Kelvin, with K = 273.15 + degree in Celsius
KP	Gas permeability through the packaging film ($cm^3\ \mu m^{-1}\ m^{-2}\ d^{-1}\ bar^{-1}$)
l	Cheese thickness (m)
M	Molar mass (kg/mol)
p	Partial pressure (Pa)
P_T	Total pressure (atm)
Pe	Gas permeability through the packaging film ($mol\ m^{-1}\ s^{-1}\ Pa^{-1}$)
PAB	Propionic Acid Bacteria
pred	Predicted values
PTATN	ratio of phosphotungstic acid soluble nitrogen on total nitrogen (g/100g)
S or SCO2	Solubility coefficient of CO_2 in cheese ($mol\ m^{-3}\ Pa^{-1}$ or $mmol\ kg^{-1}\ atm^{-1}$) or CO_2 solubility
SM	Salt in moisture ratio (g/100g)
t	Time (s)
T	Temperature (K)
R	Universal gas constant: 8.314 ($J\ mol^{-1}\ K^{-1}$)
CVRMSD	Coefficient of variation of the root mean squared deviation
V	Volume (m^3)
x	Position in the cheese (m)
y	Experimental or predicted variable
μ	average
$\boldsymbol{\varphi}$	Mass flow ($kg\ s^{-1}$)
ν	Production rate ($kg\ m^{-3}\ s^{-1}$)
∞	Relative to the surrounding atmosphere

26

1. Introduction

In food engineering, mathematical modelling of physical mechanisms such as heat or mass transfer was used for many years to simulate and optimize/control operation units such as drying or salting (Bona et al., 2007; Mayor and Sereno, 2004; Payne and Morison, 1999; Santapaola et al., 2013). More recently these models were coupled to biological ones such as Mickaëlis Menten equation that formalize the aerobic respiration (Ho et al., 2011; Guillard et al., 2012), chemical reaction for oxidation (Bacigalupi et al., 2013) or predictive microbiology models in order to better represent the evolution of the packed food during storage (Chaix et al., 2015).

This modelling approach coupling equations coming from different disciplinary fields was recently applied to semi-hard Swiss-type cheese in order to model the eyes' growth during ripening (Laridon, 2014; Laridon et al., 2016). CO_2-source in this type of cheese is propionic acid bacteria (PAB) which means that CO2-production rate and amount in such cheese is much higher compared to that of lactic acid bacteria. The ripening of these cheeses includes a step during which cheeses are stored at warm temperature (about 1-2 weeks at 20-25°C) for stimulating the PAB fermentation. During this step, CO_2 is intensively produced, leading to the growth of eyes (Fröhlich-Wyder and Bachmann, 2004). Cheeses are often foil ripened and a plastic packaging is used to wrap the cheeses during the whole ripening period for avoiding excessive loss of gaseous compounds. The modelling approach proposed by Laridon (2014) therefore concomitantly took into account mass transfer of gas (CO_2 produced by bacteria and responsible of eyes' growth), production of the CO_2 and mechanical constraint imposed to cheese paste by this production. This model was based on experimentally assessed rheological parameters (stress) and CO_2 production rate in simplified condition, but some input parameters such as CO_2 diffusivity and solubility into the cheese were estimated from the literature and assumed constant throughout the cheese paste and the ripening age. The sensitivity analysis performed by these authors revealed

afterwards the higher influence of CO_2 production and diffusion parameters compared to the rheological ones in semi-hard cheese (Laridon, 2014).

Faced to the importance of CO_2 diffusion and CO_2 production rate in the ripening of semi-hard Swiss-type cheese, this paper aimed at deepening these two phenomena by coupling them in a mathematical model in order to simulate and predict evolution with time of CO_2 gradients in the cheese paste and in the packed cheese (including CO_2 permeation through the ripening foil). In this purpose, the aim of this study was to develop and experimentally validate in various conditions, mimicking the ripening conditions of Swiss-type cheese, a mathematical diffusion-reaction model to predict CO_2 gradients in packed cheeses during ripening.

2. Materials and methods

2.1 Cheese and packaging

Semi-hard cheese blocks of 1 kg were kindly supplied by a cheese company. The cheeses included about 42% w/w moisture and 26.5% w/w fat, with pH varying from 5.50 to 5.70 from 14 to 28 days from renneting. The cheeses used for the model validation without CO_2 production (same batch) did not include any intentionally added CO_2 producing bacteria (PAB and hetero-fermentative lactic acid bacteria or LAB) and was produced from pasteurized milk to avoid any sources of hetero-fermentative LAB or PAB. The cheeses used for the validation with CO_2 production included PAB (10^6 CFU ml^{-1} cheese milk) as main source of CO_2 production. They were produced from a second, dedicated batch from pasteurized milk. After brining, all cheeses were packed in a multilayer barrier packaging film made of PE/PVDC/PE. Indicatively, the permeability to CO_2 at 19°C equalled 40000 cm^3 µm m^{-2} d^{-1} bar^{-1} (Acerbi et al., 2016c). The ripening schedule of all ripened cheeses was as follows: 13°C until 14 days from renneting, 19°C

for 14 days, 2–3 days at 13°C, longer storage at 6°C. The target chemical composition of cheeses used in this study is described in Table 1.

Cheese blocks were about 15 to 8 cm square in shape (see Supplementary Material A) and were sampled in their core, orthogonally to the interface exposed to headspace/surrounding atmosphere (Figure 1), at least 3 cm away from side rinds, resulting in a cylinder of 8 cm height and about 2 cm of diameter. The sampling region was then cut in thin slices of minimum 0.5 cm of thickness for assessment of chemical composition gradient or CO_2 gradient.

Table 1

2.2 Chemical analyses

The chemical composition (fat, moisture, pH, total nitrogen (TN) and fractions of TN, salt, organic acids) of three cheeses per production was measured, in order to verify that the cheese production was on target. Dry matter and sodium chloride were measured according to the ISO 5534 (Anonymous, 2004a) and ISO 5943 (Anonymous, 2006) standards. Total nitrogen (TN), water soluble nitrogen (SN) and phosphotungstic acid soluble nitrogen (PTA-N) were measured using Kjeldahl based methods according to ISO 8968-3 standard (Anonymous, 2004b; Bütikofer et al., 1993). The ratio of PTA-N on TN (g/100g) was considered as a good proteolytic indicator. pH and fat content were characterized according to respectively, FD V04-035 (Anonymous, 2009) and NF V04-287 (Anonymous, 2002) French standards. Organics acids were assayed using internal method based on high-performance liquid chromatography.

CO_2 determination in cheese was carried out with the protocol described in Acerbi et al. (2016b). The protocol included a first step where CO_2 was extracted from the cheese sample by immersing it in acidic solution. The extracted CO_2 was then scavenged by a soda solution of known

molarity, which was finally titrated with hydrochloric acid. The difference between the initial and final soda molarity related to the moles which reacted with CO_2.

2.3 Microbiology analyses

Propionic acid bacteria were enumerated with a method based on the count of the diluted colonies grown on agar plates enriched mainly with sodium lactate and yeast extract after 1 week of incubation at 30°C. The results were expressed in colony-forming unit per gram of cheese (CFU g^{-1}).

2.4 Gas chromatography for headspace analyses

The partial pressure of N_2, O_2 and CO_2 was measured (resolution: 0.005%) by injecting 10 µl of headspace of cheese packs inside a micro gas chromatography unit including a thermal conductivity detector (MicroGC 3000, SRA Instruments). Homogeneity of the gas composition was ensured by pumping few millilitres of sample gas inside the micro gas chromatography unit before each measurement. The cheese packs were not kept after the analyses because of the too low amount of headspace volume. Therefore, new cheese packs produced from the same batch were used for each analysis in order to follow the kinetics of headspace composition during ripening. The gas chromatography unit was previously calibrated with gas bottles of known compositions. At least two measurements were carried out per each sample.

2.5 Description of the model

Evolution of CO_2 partial pressures in the foil packed blind cheese during ripening relies on the interplay of four mechanisms: (1) CO_2 production due to the activity of microorganisms (PAB), (2) gas transport within the cheese paste, (3) gas transfer at the cheese rind/headspace interface and (4) gas transmission through the packaging film. The four described mechanisms are illustrated in figure 1.

121

122 **Figure 1**

123

124 **2.5.1 Model assumptions**

125 The following assumptions were made in the present mono-directional modelling study:

126 - The composition of the atmosphere surrounding the packed cheese during ripening is
127 constant and equals to 78.1% for N_2, 20.9% for O_2 and 0.03% for CO_2 (Widory and
128 Javoy, 2003).

129 - Temperature in the packed cheese system and surrounding atmosphere is constant,
130 without gradients.

131 - Total pressure of the system is constant and it equals atmospheric pressure (101325 Pa).

132 - The solubilization of N_2 inside the cheese was considered negligible compared to CO_2,
133 because of its lower solubility in water (about 50 times less soluble than CO_2 in water at
134 20°C) (Dean, 1999). O_2 solubility and diffusivity in the cheese were set to constant values
135 of 2.5 10^{-9} m^2 s^{-1} and 1.3 mmol kg^{-1} atm^{-1} respectively and which correspond to solubility
136 and diffusivity of the gas in water at 20°C (Chaix et al., 2014).

137 - The mechanical resistance to deformation of the cheese packaging is not taken into
138 account in the model. Thus, volume changes according to moles content inside the pack
139 and total pressure of headspace remains equal to external atmospheric pressure.
140 Measuring volume changes during experiment has revealed that they are negligible and
141 that the flexible pouch could easily compensate the small volume change due to its
142 property of elongation.

- For the cheese with salt gradient, the initial NaCl gradient was measured in cheeses produced within the same production day and it was considered to remain constant during the experiment. Same assumption was used to quantify the proteolytic indicator (PTATN).
- Gradients in chemical composition in the cheese from its upper rind to its core are symmetric to the gradients from lower rind to the core.

2.5.2 Gas balance in headspace

The variation of concentration of the gas species j in the packaging headspace HS depends on the mass flow of gas permeating the packaging film f from the surrounding atmosphere φ_{j_f} (kg/s) and the mass flow of the gas species occurring at the interface between the cheese and the headspace φ_{j_I}.

Assuming that the packaging film does not oppose any mechanical resistance to deformation, when the amount of gas species in the headspace varies, the headspace volume V_{HS} (m^3) changes, whereas the total pressure in the headspace P_T remains constant and equal to atmospheric pressure (101325 Pa). The global mass balance of species j in the headspace can hence be written as follows:

$$V_{HS}\frac{dC_{j_{HS}}}{d_t} + C_{j_{HS}}\frac{dV_{HS}}{d_t} = \varphi_{j_f} + \varphi_{j_I} \quad \text{(Eq. 1)}$$

where $C_{j_{HS}}$ (kg/m^3) is the concentration of the gas in the headspace and t is time (s).

Assuming that the gas mixture in the headspace obeys the ideal gas law, $\frac{dV_{HS}}{d_t}$ can be calculated as a pondered sum of the different aforementioned mass flow φ_{j_f}, φ_{j_I} as follows:

$$\frac{dV_{HS}}{d_t} = \frac{RT}{P_T}\left(\frac{\varphi_{CO2_f}+\varphi_{CO2_I}}{M_{CO2}} + \frac{\varphi_{O2_f}+\varphi_{O2_I}}{M_{O2}} + \frac{\varphi_{N2_f}}{M_{N2}}\right) \quad \text{(Eq.2)}$$

where M_j is the gas molar mass (kg/mol), R the universal gas constant (J mol^{-1} K^{-1}) and T the temperature in Kelvin (K).

The concentration of the gas in the headspace $C_{j_{HS}}$ can be calculated according to (Eq. 3)

$$RT \sum_{j=\{O_2,CO_2,N_2\}} \frac{C_{j,HS}}{M_j} = P_T = 10^5 Pa \quad \text{(Eq. 3)}$$

and similarly, for the partial pressure of the gas in the headspace $p_{j_{HS}}$ (Eq. 4),

$$p_{j_{HS}} = \frac{C_{j_{HS}} R T}{M_j} \quad \text{(Eq. 4)}$$

2.5.3 Gas permeation through the maturation foil

The gas permeation through the packaging film (maturation foil), assuming that the partial pressures in the atmosphere surrounding the cheese are constant, could be conveniently described by the Fick's first law (steady state regime). Therefore, the mass flow φ_f of gases j (N_2, O_2, CO_2) through the packaging film was calculated according to first Fick's law (Fick, 1855) as stated in Eq. 5.

$$\varphi_{j_f} = M_j Pe_j \frac{A_f}{l_f}\left(p_{j_\infty} - p_{j_{HS}}\right) \quad \text{(Eq. 5)}$$

where Pe_j is the permeability coefficient of the gas j through the film (mol m^{-1} s^{-1} Pa^{-1}), l_f is the thickness of the film (m), A_f is the film surface (m^2) and p_{j_∞} and $p_{j_{HS}}$ are the partial pressure of the gas j in the surrounding atmosphere (denoted by symbol ∞) and the packaging headspace, denoted by HS.

2.5.4 Mass flow at the cheese rind/gaseous interface

The mass flow at the cheese/rind gaseous interface was calculated as follows (Eq. 6):

$$\varphi_{j_I} = kj\left(\frac{M_j A_I}{RT}\right)\left(p_{j_{HS,I}} - p_{j_{HS}}\right) \quad \text{(Eq. 6)}$$

Where k(m/s) is the mass transfer coefficient at the interface between the cheese rind and the headspace and A_I and $p_{j_{HS,I}}$ are the surface at the interface and the partial pressure at the

immediate vicinity of the cheese surface. The mass transfer coefficient k is calculated according to Eq. 7

$$kj = \frac{Bi \times D_j}{L} \quad \text{(Eq. 7)}$$

Where Bi is the non-dimensional Biot number, assumed to be equal to 10^5 (ratio between diffusivity of CO_2 in air and cheese) (Laridon, 2014), D_j is the diffusivity of CO_2 in cheese (about 10^{-10} m^2 s^{-1}) and L is the characteristic length of the considered material (length of the cheese equalled about 0.008m).

Assuming that the gaseous species in headspace are in thermodynamic equilibrium with the dissolved species at the cheese surface, the concentration of dissolved gas species j at the cheese surface $C_{j_{ch,x=0}}$ (kg/m^3) relates to $p_{j_{HS,I}}$ according to Henry's law:

$$p_{j_{HS,I}} = \frac{C_{j_{ch,x=0}}}{M_j S_j} \quad \text{(Eq. 8)}$$

Where S_j is the solubility coefficient of the considered gas j (mol m^{-3} Pa^{-1}).

2.5.5 Gas diffusion inside the cheese paste and CO_2 production

The CO_2 diffusion within the cheese paste was represented by making use of Fick's second law of diffusion for the transient state of diffusion and it was coupled to CO_2 production by adding production term ν (kg m^{-3} s^{-1}) to Fick's second law, leading to Eq. 9.

$$\frac{\partial c_{CO_2 ch}}{\partial t} = D_{CO2} \frac{\partial^2 c_{CO_2 ch}}{\partial x^2} + \upsilon_{CO2} \quad \text{(Eq. 9)}$$

Where $\frac{\partial c_{CO_2 ch}}{\partial t}$ is the partial derivative of the concentration of CO_2 in the cheese as regard to time, in the direction x (m). x represents the distance from the interface of the cheese rind to headspace and the considered position inside the cheese. x varies from 0 to 8 (cheese thickness in cm). D_{CO2} is the effective diffusivity coefficient of CO_2 in cheese (m^2/s).

The same equation without the production term was used to model O_2 diffusion within the cheese paste.

2.5.6 Boundary conditions

Equality of flows was considered at the interface between the cheese rind and the headspace:

$$D_j \frac{\partial c_{j_{ch}}}{\partial x} = \frac{\varphi_{j_I}}{A_I} = kj\left(\frac{M_j}{RT}\right)\left(p_{j_{HS,I}} - p_{j_{HS}}\right) \; at \; x = 0 \qquad \text{(Eq. 10)}$$

where j stands for either CO_2 or O_2.

Since the cheese is pressed on continuous impermeable material during ripening due to gravity, we assumed no diffusion at the cheese bottom rind (br), ($x = br$):

$$D_j \frac{\partial c_{j_{ch}}}{\partial x} = 0 \; at \; x = br \qquad \text{(Eq. 11)}$$

Assuming that the food sample was initially in equilibrium with a gas of fixed partial pressure p_{j_0} (Pa), the initial conditions take the form:

$$C_{j_{ch}}(x, 0) = M_j Sj \; p_{j_0}(x, 0) \quad for \; t = 0 \qquad \text{(Eq. 12)}$$

2.5.7 Prediction of model input parameters for different ripening conditions

The following empirical equation was used in the model for predicting the changes in CO_2 production rate, υ_{CO2} (mmol kg^{-1} d^{-1}) as a function of salt to moisture ratio, SM and temperature, T (Acerbi et al., 2016a):

$$\upsilon_{CO2} = 8.527 + 0.0862\ \mathrm{T}^2 - 1.621\ \mathrm{T} + 5.367\ \mathrm{SM} - 0.415\ \mathrm{SM\ T} \qquad \text{(Eq. 13)}$$

SM (g/100g) is calculated as the percentage of the mass ratio between sodium chloride and moisture.

The following empirical equation was used in the model for predicting the value of D_{CO2} at different temperatures, T salt to moisture ratio, SM and $PTATN$ (ratio of phosphotungstic acid soluble nitrogen on total nitrogen). The latter coefficient is a ripening indicator related to the

proteolytic phenomena (especially amount of free amino acids) which relates to structure changes in the cheese during ripening (Acerbi et al., 2016d).

$$D_{CO2} = (-0.0428\,\mathrm{T}^2 + 1.3689\,\mathrm{T} - 0.6188\,\mathrm{SM} + 12.2421\,\mathrm{PTATN} - 9.6910) \times 10^{-10} \quad \text{(Eq. 14)}$$

The value of S_{CO2} (in mmol kg^{-1} atm^{-1}) was calculated by using a modified version of the equation given by Acerbi et al. (2016b):

$$S_{CO2} = 37.35879 - 0.83414\,SM^2 + 4.4619\,SM - 0.34768\,T \quad \text{(Eq. 15)}$$

The modification consisted in the use of a quadratic term for the salt effect instead of a linear term in the view of more recent results (figure 2).

Figure 2

The value of permeability *(KP)* of the gas j (O_2 CO_2, N_2) was estimated at different ripening temperatures by interpolating the results of permeability coefficients KP given by Acerbi et al. (2016c) in units cm^3 µm m^{-2} d^{-1} bar^{-1}. The KP values were converted into Pe values (mol m^{-1} s^{-1} Pa^{-1}) to be used in the model (Eq. 5).

$$KP_{CO2} = -108.03\,T^2 + 4551.5\,T - 3242.6 \quad \text{(Eq. 16)}$$

$$KP_{O2} = 386.53\,T + 6313.6 \quad \text{(Eq. 17)}$$

$$KP_{N2} = 188.78\,T + 3422 \quad \text{(Eq. 18)}$$

2.5.8 Numerical solving and identification procedure

This system of equations governing the coupled diffusion and production of gas in the cheese and the gas transfer and permeation in the cheese packaging headspace was solved using a dedicated algorithm “ode15s” developed in Matlab® computing software (The Mathworks Inc., Natick,

Mass, USA) and adapted to stiff systems where each of unknown variables may exhibit radically different variation kinetics. This algorithm adjusted automatically the size of the time step used for numerical integration of the equations. To evaluate goodness of fit between experimental and predicted data, the coefficient of variation of the root mean square deviation (CVRMSD) was calculated as follows:

$$CVRMSD = \left(\frac{\sqrt{\frac{(ypred-yexp)^2}{(N)}}}{\mu_{exp}}\right) \times 100 \quad \text{(Eq.19)}$$

Where y_{pred} and y_{exp} are respectively the experimental and the simulated residual value, N is the number of experimental measurements and μ_{exp} is the average of the experimental values. CVRMSD enables to compare the quality of the model with other models present in literature. A good quantitative model is considered to have CVRSMD ≤ 10%.

2.6 Model validation

The experimental validation was made in three steps of increasing complexity which are summarized in Table 1.

❶ Firstly, the mono-directional CO_2 diffusion within the cheese and transfer at the cheese rind interface was validated on an old ripened high salted cheese (namely “old cheese”) with no salt gradient and without CO_2 production (no CO_2 producing bacteria). The cheese was high salted via brining (about 5% NaCl/dm, salt content on dry matter) in order to avoid possible gas production from unwanted microorganisms in such old cheese. The cheese, apart for its upper rind, was fully covered with a gas impermeable membrane (see Supplementary Material A) and it was housed in a controlled temperature cabinet (set at 19°C) with a continuous flow of wet CO_2 (gas supposed to be equilibrated at 100% of relative humidity after bubbling in a flask containing pure water at the temperature of the experiment). After 3 days, the CO_2 dissolved in different positions (e.g. the sample is sliced parallel to the interface) from the upper rind (x=0) to the

bottom rind (x=8) was assessed with the CO_2 determination method described above. Two repetitions were made in order to validate the diffusion phenomenon. For two other repetitions, after 3 days of CO_2 sorption, the cheese samples were then kept 3 days in a continuous flow of wet (100% RH) N_2 (desorption step). The gradient of dissolved CO_2 into the paste after these 3 days of desorption was then assayed as previously described for the sorption step (2 repetitions).

❷ Secondly the coupling of CO_2 diffusion and production was experimentally assessed by using a cheese with PAB and average salt concentration (about 2.5% NaCl/dm, salt on dry matter, in the cheese, namely "young cheese"). This cheese also included a salt gradient due to its younger age (15 days from renneting) when salt is still slowly diffusing from rind to core of the cheese (brined cheese). The same experimental procedure previously described was used, apart for the following: the cheese stayed 1 day at 19°C, before the experiment with the contact of wet CO_2 from upper rind (x=0) started and it lasted for 4.4 days.

The initial CO_2 concentration gradient in the cheese was measured just before the experiment started (i.e. about 9.5 weeks from renneting for the first validation step and 15 days from renneting for the second more complex validation step including CO_2 production). This initial CO_2 gradient is indispensable to parametrize initial conditions in the numerical algorithm.

❸ Thirdly, in order to compare the output of gas concentration in the headspace given by the model including permeation phenomenon, gas headspace composition was measured in the headspace of packed cheeses (2 replications). The headspace gas analyses were repeated on different cheeses during ripening (about at 10, 14, 16 ripening days at 19°C).

In each case of these aforementioned steps, the model was adapted accordingly to experimental conditions: system of Eq. (6) to (15) for the first and second steps - without the production term in Eq. (9) and related Eq. (13) – and system of Eq. (1) to Eq. (18) for the third, full case.

299

300 **2.7. Statistics**

301 Statistical tests were performed by using R software for statistical computing (R, 2014).
302 Comparisons between the chemical compositions were performed by pairwise comparisons using
303 *t* test with pooled standard deviation. The Holm method for the multiplicity of error was used to
304 adjust the p-value of multiple pairwise comparisons. Different letters were used for denoting
305 significant difference between data sets (level of significance $\alpha = 0.05$, unless stated).

306

307 ## 3. Results and discussion

308 Our model takes into account experimentally assessed parameters for describing CO_2 production
309 and overall transfer in and out a cheese/packaging system during foil ripening. The focus was on
310 the exhaustive description of the gas transport properties in the continuous cheese paste and at its
311 interface with the surrounding atmosphere. We therefore used a model blind cheese (without
312 eyes). We experimentally assessed the following parameters: transport of CO_2 in the cheese paste
313 (effective diffusivity), transfer of CO_2 at the interface between cheese and headspace (solubility),
314 oxygen, nitrogen and carbon dioxide transmission rate through the maturation foil (permeability)
315 and CO_2 production rate from the bacteria. The cited parameters were previously assessed in
316 function of the main ripening variables (different temperatures, ripening time, salt content
317 amongst others) (Acerbi et al., 2016a, 2016b, 2016c, 2016d).

318

319 **3.1 Compositional analyses**

320 The chemical composition of the cheese without PAB (old cheese – data not shown) was not
321 significantly different (α=0.05) as a function of the position in the cheese, whereas a relevant
322 gradient in PTATN (ratio of phosphotungstic acid soluble nitrogen on total nitrogen) and SM

(salt in moisture ratio) was confirmed from analyses made on cheese with PAB analysed at 15 and 20 days from renneting (figure 3).

Although the transfer properties of nitrogen components (PTATN) and salt were not experimentally assessed within this study and not included in the model, the initial heterogeneous composition was considered and a linear interpolation was used for predicting the initial composition in all positions of the cheese including PAB. The composition in the position 4 to 8 cm was considered symmetrical to the position 0 to 4 cm.

Figure 3

A relevant gradient in organic acid concentration was found in the cheese with PAB both at 15 and 20 days from renneting (figure 4). No propionate and acetate was found in the outer rind (0 cm) at 15 days from renneting. The observed delay in PAB fermentation in the outer part of the cheese was probably due to the negative effect of high salt to moisture ratio on the bacteria cells (Guinee, 2004) and it was already demonstrated by Huc et al. (2014) in similar cheeses. The molar ratio between propionate and acetate in the core of the cheese equalled about 2. The ratio of 2 is obtained if PAB convert lactate exclusively via the Fitz pathway (Fröhlich-Wyder and Bachmann, 2004; Piveteau, 1999; Fedio et al., 1994). We can therefore confirm that, in the studied cheese, PAB fermented lactate primarily via the Fitz pathway and that probably no other metabolic activity (producing acetate) occurred.

Figure 4

The pH of the cheese was measured because pH changes may affect both the solubility of carbon dioxide dissolved in the water phase of the cheese (Chaix et al., 2014) and its diffusivity coefficient due to a different organisation of the casein matrix structure (Lawrence et al., 1987). The pH in the studied cheese did not relevantly vary in the considered experimental time (figure 5a).

The enumeration of PAB cells confirmed the higher metabolic activity observed in the core of the cheese (figure 5b).

Figure 5

3.2 Initial CO_2 concentration

The initial CO_2 concentration in different positions (from upper to bottom rind) of the cheese was measured in 2 to 3 cheeses produced within the same production batch. Whereas the CO_2 distribution was low and rather homogeneous for the old ripened cheese with no intentionally added CO_2 producing bacteria (figure 6a, 3 repetitions), the initial CO_2 gradient was relevant in the cheese with PAB (figure 6b, 2 repetitions). The low and homogeneous initial CO_2 concentration observed in the older cheese was expected because this cheese did not contain intentionally added CO_2 producing bacteria, while the CO_2 gradient observed in the cheese with PAB at 15 days from renneting (14 days at 13°C and 1 days at 19°C) reflected the effect of salt gradient on PAB. There is an inhibition of PAB growth (Figure 5b) by the higher salt content close to the rinds with a consequently lower production of CO_2 and propionic acid close to the rinds compare to the core of the product leading to this “bell like curve” for initial CO_2 gradient in salted cheese with PAB. This evolution of salt content that is spatially-dependant, due to diffusion of salt from the periphery towards the centre of cheeses, has been found in previous

studies (Huc et al., 2014; Guinee, 2004; Hollywood & Doelle, 1984) and before by Mocquot (1979), Geurts et al. (1974, 1980) and Pauchard et al. (1980). Therefore, the median value for initial CO_2 concentration was used (4 mmol/kg) for the model validated for the cheese without PAB and the real gradient was used as input vector for initial CO_2 concentration for the cheese with PAB.

Figure 6

3.3. Investigating effect of salt content on CO2 solubility

Prior model validation, additional points of solubility of CO_2 within the cheese paste were measured to complete the work of Acerbi et al. (2016b) and obtain more precise S_{CO2} prediction (eq. 15). According to these new values (Figure 2), S_{CO2} increased with light NaCl content, while it decreased at very high NaCl content, following a similar behaviour compared to salting in and salting out effect of protein. This phenomenon was ascribed to the possibly higher sorption of CO_2 in highly hydrated protein during salting in phase (Guinee, 2004), while the overall S_{CO2} would decrease due to lower level of protein hydration at high salt concentration (salting out). Guinee (2004) suggested that salting out effect of protein in cheese (Mozzarella) may take place for salt to moisture ratio (S/M) higher than 6.3% w/w, which is close to the highest salt level investigated in Figure 2 (about 6.7% S/M).

3.4 Model validation

The simplest model form describing CO_2 diffusion inside the cheese paste (without PAB and CO_2 production) and the transfer at the cheese rind/gaseous interface (100% CO_2) was successfully validated because the difference between predicted and experimental data was below 10% (figure

393 7a). Same good validation with a 100% N_2 flux at the cheese rind surface was obtained
394 (CVRMSD < 8%) (see Supplementary Material B).
395 When increasing the complexity of the model, including CO_2 production rate and considering a
396 cheese with salt gradient, the observed error between experimental and predicted data was found
397 higher (30%) (figure 7b). In the latter more complex model, the predicted line was generally
398 underestimating the experimental gradient, leading to a high CVRMSD. The lack of fit of the
399 more complex model could be due to (1) the adoption of a mono-directional model which may
400 not be fully appropriate for diffusion in cheeses with gas production and/or (2) underestimations
401 in either the prediction of CO_2 production rate and/or in the initial CO_2 concentration gradient.
402 Underestimation of the CO_2 production rate may be due to the linear approximation used by
403 Acerbi et al. (2016a) to describe the effect of salt content. Indeed, lower salt contents were
404 investigated in the previous work, which provided the predictive equation for CO_2 production
405 rate, compared to the current study. Therefore, effect of high SM ratio is probably not well
406 predicted by Eq.13 which was never validated for such SM ratio. This underestimation may be
407 overcome by carrying out more experimental measurements of CO_2 production rate at higher salt
408 content. A possible underestimation of the initial CO_2 concentration gradient in the cheese may
409 be ascribed to natural deviations in metabolic activity of the PAB in different cheeses produced
410 from the same batch. Both hypotheses were confirmed by simulating a 1.7 folds higher CO_2
411 production rate (figure 8) and then, a 2 folds higher initial CO_2 concentration (figure 9). In both
412 cases, the predicted curve fit very well the experimental data.
413
414 **Figure 7**
415
416 **Figure 8**

417

418 **Figure 9**

419

420 Then, the full model considering permeation through ripening foil in addition to
421 solubilisation/diffusion and production of CO_2 within the food was then used to predict the CO_2
422 partial pressure in headspace. A third set of experiments conducted on cheeses packed in ripening
423 foils were conducted in the objective to validate it. Experimental difficulties arose because gas
424 headspace analysis could not be assessed continuously in the pack (because of too high gas
425 volume injected) therefore only a few experimental points have been collected (See
426 supplementary material C). However, it has been noted that the model tended to underestimate
427 the headspace partial pressure when CO_2 production occurs (in cheese with PAB). But, once
428 again, considering a 1.7 fold higher CO_2 production rate, the prediction fitted better the
429 experimental data. A better fit may also be obtained by reducing the value for CO_2 permeability
430 of the packaging or increasing the initial CO_2 concentration gradient (results not shown). But this
431 hypothesis does not sound well founded and therefore was not applied. The permeability values
432 were especially assessed in the conditions encountered in the present work and were therefore
433 considered relevant.

434 **3.5 Exploratory analysis of model simulations**

435 Simulations were carried by considering the min and max values of 4 parameters in their range of
436 variation (table 2): CO_2 solubility (figure 10a), diffusivity (figure 10b), permeability (figure 10c)
437 and production coefficients (figure 10d). During the simulation, only one of the mentioned input
438 parameters was varied from the lowest to the highest value described in Table 2. The boundary

conditions used during these simulations included that the packed cheese was in contact with the atmosphere (20.9% O_2, 0.03% CO_2, 78.1% N_2) from one rind (upper rind) and in contact with a non-permeable support from the below rind (shelf). The range of values for solubility and diffusivity was chosen in agreement with the min and max observed in the experimental campaign described by Acerbi et al. (2016b, 2016d). The values for permeability were decided to vary of factor 10 of the predicted value of Equation 16, 17, 18. The value of production rate was decided to vary of 4 units compared to the predicted value of equation 13, because it was considered a realistic variation for the different salt contents observed in different positions of the studied cheese at 19°C.

Table 2

The other input parameters were kept fixed (medium value) as respect of their position. This simplified sensitivity analysis had the goal of highlighting which input parameter had the strongest effect on the output (CO_2 gradients formed in cheese). Logically, changing S_{CO2} led to light differences in CO_2 concentration only close to the gaseous interface (figure 10a) because this parameter only intervenes in the boundary condition at cheese/headspace interface: the lower the solubility, the lower the CO_2 content at the interface. Changing D_{CO2} slightly affected the shape of the CO_2 gradient close to the cheese rinds, probably because these positions were characterized by lower υ_{CO2} due to the higher salt content (figure 10b) and it affected the overall shape of the curve. υ_{CO2} showed the highest effect on the CO_2 gradients, from -10 to +20 mmol/kg of difference for the lowest and highest υ_{CO2} respectively compared to the median value in the core of the cheese. Concerning the effect of different permeability, the lower the gas

462 permeability of the packaging, the higher was the CO_2 concentration at the cheese rind, but the
463 overall change in CO_2 gradient due to different permeability was negligible.
464
465 **Figure 10**
466
467 This paper presents an unprecedented modelling approach that successfully describes the
468 mechanisms of CO_2 diffusion, solubilisation and production by Swiss-type cheese with intensive
469 PAB-based CO_2 production and also CO_2 permeation through the ripening foil. All mechanisms
470 were dynamically coupled and experimentally validated permitting to achieve the initial objective
471 of this paper which was to predict evolution with time of CO_2 gradients into the packed cheese.
472 The developed model is the most complete one compare to precedent similar approach of the
473 literature. For instance, the one of Jakobsen and Risbo, (2009), developed for prediction, among
474 others, of the changes in solubilised carbon dioxide in semi-hard cheese packed in modified
475 atmosphere packaging, neglected all mechanisms of CO_2 diffusion and production in their
476 approach.
477 This model could be further used to predict CO_2 gradients into blind cheese or, once coupled with
478 a mechanical model of bubble growth such as the one proposed by Laridon et al., (2014), could
479 be used to predict eye growth in Swiss type cheese and then pilot the ripening step.
480

481 ## 4. Conclusion

482 We presented the first experimentally validated model which couples the phenomena of CO_2
483 production, solubilisation/diffusion and permeation in a packed cheese system for predicting the
484 CO_2 gradients formed in the cheese during ripening. A three steps validation procedure enabled
485 to build a robust model for a quantitative description of CO_2 gradient formed in a cheese with or

without CO_2 production by PAB and including the phenomena of CO_2 diffusion in the cheese paste and transfer at the gaseous interface. The model was able to describe the shape of the CO_2 gradient formed in the cheese with, nevertheless, less precision when CO_2 production happens. This term was probably less accurately characterized for the conditions used in this paper and induces less performant prediction. A simplified sensitivity analysis highlighted CO_2 production as the most important input parameter affecting the CO_2 gradients formed in cheese during ripening. Results presented in this paper represent a solid basis for the description of the most important phenomena affecting the quality of cheese with intense CO_2 production during ripening.

References

Anonymous 2004a. ISO 5534. Cheese and processed cheese -- Determination of the total solids content (Reference method). International Organization for Standardization, Geneva

Anonymous 2004b. ISO 8968-3. Milk -- Determination of nitrogen content -- Part 3: Block-digestion method (Semi-micro rapid routine method). International Organization for Standardization, Geneva

Anonymous 2006. ISO 5943. Cheese and processed cheese products -- Determination of chloride content -- Potentiometric titration method. International Organization for Standardization, Geneva

Anonymous 2009. FD V04-035. Lait et produits laitiers - Détermination du pH. Afnor, France

Anonymous 2002. NF V04-287. Fromages - Détermination de la teneur en matière grasse - Méthode acido-butyrométrique, Afnor, France

Acerbi, F., Guillard, V., Aliani, M., Guillaume, C., Gontard, N., 2016a. Impact of salt concentration, ripening temperature and ripening time on CO2 production of semi-hard cheese with propionic acid fermentation. J. Food Eng. 177, 7279. doi:http://dx.doi.org/10/2016/j/jfoodeng.2015.12.022

Acerbi, F., Guillard, V., Guillaume, C., Gontard, N., 2016b. Impact of selected composition and ripening conditions on CO2 solubility in semi-hard cheese. Food Chem. 192, 805–812. doi:10.1016/j.foodchem.2015.07.049

Acerbi, F., Guillard, V., Guillaume, C., Gontard, N., 2016c. Assessment of gas permeability of the whole packaging system mimicking industrial conditions. Food Packag. Shelf Life 8, 81–85. doi:https://doi.org/10.1016/j.fpsl.2016.04.003

Acerbi, F., Guillard, V., Guillaume, C., Saubanere, M., Gontard, N., 2016d. An appraisal of the impact of compositional and ripening parameters on CO2 diffusivity in semi-hard cheese. Food Chem. 194, 1172–1179. doi:10.1016/j.foodchem.2015.08.020

Bacigalupi, C., Lemaistre, Marie Hélène Peyron, S., Guillard, V., Chalier, P., 2013. Changes in nutritional and sensory properties of orange juice packed in PET bottles: an experimental and modelling

519 approach. Food Chem. 141, 3827–3836.

520 Bona, E., Silva, R. S. S. F. d., Borsato, D., Silva, L. H. M., & Fidelis, D. A. d. S. (2007). Multicomponent
521 diffusion modeling and simulation in prato cheese salting using brine at rest: The finite element
522 method approach. *Journal of Food Engineering, 79*(3), 771-778.
523 doi:10.1016/j.jfoodeng.2006.02.041

524 Bütikofer, U., Ruegg, M., Ardo, Y., 1993. Determination of nitrogen fractions in cheese: evaluation of a
525 collaborative study. Food Sci. Technol. - Leb. - Wiss. Technol. doi:10.1006/fstl.1993.1056

526 Chaix, E., Couvert, O., Guillaume, C., Gontard, N., & Guillard, V. (2015). Predictive Microbiology Coupled
527 with Gas (O2/CO2) Transfer in Food/Packaging Systems: How to Develop an Efficient Decision
528 Support Tool for Food Packaging Dimensioning. *Comprehensive Reviews in Food Science and*
529 *Food Safety, 14*(1), 1-21. doi:10.1111/1541-4337.12117

530 Chaix, E., Guillaume, C., & Guillard, V. (2014). Oxygen and Carbon Dioxide Solubility and Diffusivity in
531 Solid Food Matrices: A Review of Past and Current Knowledge. *Comprehensive Reviews in Food*
532 *Science and Food Safety, 13*(3), 261-286. doi:10.1111/1541-4337.12058

533 Dean, J. A. (1999). Physical Properties. Solubilities of gases in water. In J. A. Dean (Ed.), *Lange's Handbook*
534 *of Chemistry* (15 ed., pp. 375-380): McGraw-Hill Inc.

535 Fedio WM, Ozimek L, Wolfe FH. 1994. Gas production during the storage of Swiss cheese.
536 Milchwissenschaft-Milk Science International 49(1):3-8.

537 Fick, A., 1855. On liquid diffusion. J. Memb. Sci. 100, 33–38.
538
539 Fröhlich-Wyder MT, Bachmann HP. 2004. Cheeses with propionic acid fermentation. In: Fox PF,
540 McSweeney PLH, Cogan TM, Guinee TP, editors. Cheese: Chemistry, Physics and Microbiology. 3
541 ed. London: Elsevier Academic Press. p. 141-156.

542 Geurts, T. J., Walstra, P., & Mulder, H. (1974). Transport of salt and water during salting of cheese. 1.
543 Analysis of the processes involved. *Netherlands Milk and Dairy Journal*, 28,102-129.

544 Geurts, T. J., Walstra, P., & Mulder, H. (1980). Transport of salt and water during salting of cheese. 2.
545 Quantities of salt taken up of moisture lost. *Netherlands Milk and Dairy Journal*, 34, 229-254.

546 Guillard, V., Guillaume, C., Destercke, S., 2012. Parameter uncertainties and error propagation in
547 modified atmosphere packaging modelling. Postharvest Biol. Technol. 67, 154–166.
548 doi:10.1016/j.postharvbio.2011.12.014

549 Guinee, T. P. (2004). Salting and the role of salt in cheese. *International Journal of Dairy Technology,*
550 *57*(2-3), 99-109.

551 Ho, Q. T., Verboven, P., Verlinden, B. E., Herremans, E., Wevers, M., Carmeliet, J., & Nicolaï, B. M. (2011).
552 A Three-Dimensional Multiscale Model for Gas Exchange in Fruit. *Plant Physiology, 155*(3), 1158-
553 1168.

554 Hollywood, N.W., & Doelle, H.W. (1984). The effect of sampling position and age on levels of
555 propionibacteria and flavor-related compounds in Swiss-type cheese. *Australian Journal of Dairy*
556 *Technology*, 39,80-82.

557 Huc, D., Roland, N., Grenier, D., Challois, S., Michon, C., & Mariette, F. (2014). Influence of salt content
558 on eye growth in semi-hard cheeses studied using magnetic resonance imaging and CO2
559 production measurements. *International Dairy Journal, 35*(2), 157-165.
560 doi:http://dx.doi.org/10.1016/j.idairyj.2013.11.010

561 Jakobsen, M. & Risbo, J., (2009). Carbon dioxide equilibrium between product and gas phase of modified
562 atmosphere packaging systems: Exemplified by semihard cheese. *Journal of Food Engineering*.
563 92, 285–290.

564

565

566 Laridon Y., Grenier D., Houeix D., Doursat C., Lucas T., & Flick, D. (2016). Modelling of the growth of a
567 single bubble in semi-hard cheese, with experimental verification and sensitivity analysis. *Applied*
568 *Mathematical Modelling*, 40 (23-24), 1339-1351.
569 Laridon Y. (2014). Modelling and visualization of a bubble growth in an evolutive, heterogeneous
570 medium. Mechanics [physics]. University of Rennes 1. English. NNT : 2014REN1S091
571 Lawrence R. C., Creamer, L. K., & Gilles, J. (1987). Texture Development During Cheese Ripening. *Journal*
572 *of Dairy Science, 70*(8), 1748-1760.
573 Mayor, L., & Sereno, A. M. (2004). Modelling shrinkage during convective drying of food materials: a
574 review. *Journal of Food Engineering, 61*(3), 373-386. doi:http://dx.doi.org/10.1016/S0260-
575 8774(03)00144-4
576 Mocquot, B.Y.G., 1979. Reviews of the progress of Dairy Science : Swiss-type cheese. J. Dairy Res. 46,
577 133–160.
578 Payne, M. R., & Morison, K. R. (1999). A multi-component approach to salt and water diffusion in cheese.
579 *International Dairy Journal, 9*(12), 887-894. doi:http://dx.doi.org/10.1016/S0958-
580 6946(99)00157-0
581 Pauchard, J.P., Flückiger, E., Bosset, J.O., Blanc, B., 1980. CO2 Löslichkeit, Konzentration bei Entstehung
582 der Löcher und Verteilung in Emmentalerkäse. Schweizerische Milchwirtsch. Forsch. 9, 69–73.
583 Piveteau, P., (1999). Metabolism of lactate and sugars by dairy propionibacteria: A review. *Lait* 79, 23–
584 41.
585 R. (2014). R: A language and environment for statistical computing. Vienna, Austria. Retrieved from
586 <http://www.R-project.org/>.
587 Santapaola, J., Maldonado, S., & Medina, J. L. (2013). NaCl diffusion kinetics in dry salting of goat cheese.
588 *Journal of Food Engineering, 118*(2), 172-177.
589 doi:http://dx.doi.org/10.1016/j.jfoodeng.2013.03.028

590 Widory, D., Javoy, M., 2003. The carbon isotope composition of atmospheric CO2 in Paris. Earth Planet.

591 Sci. Lett. 215, 289–298. doi:10.1016/S0012-821X(03)00397-2

592

Figure 1: Scheme of the simplified food / packaging system with the four phenomena considered (mono-directional transfer through the headspace/cheese interface, *br* =cheese bottom-rind)

Figure 2. CO_2 solubility in semi-hard Swiss-type cheese as a function of salt content at 13°C. The point at intermediate NaCl content (1.5% w/w) is added to the ones reported by Acerbi et al. (2016b) and it was measured with same protocol on the same cheese. Different letters a, b c, …denote significant difference for $\alpha = 0.05$.

Figure 3. (a) PTATN - ratio of phosphotungstic acid soluble nitrogen on total nitrogen and (b) SM - salt in moisture ratio- in different positions of the of the semi-hard Swiss-type cheese with PAB, from rind (0 cm) to core (4 cm) at 15 and 20 days from renneting, representing starting time and ending time of the validation experiment.

Figure 4. Propionate (a) and acetate (b) concentrations in different positions of the semi-hard Swiss-type cheese with PAB at 15 and 20 days from renneting (young cheese).

Figure 5. pH and PAB count in different positions of the semi-hard Swiss-type cheese with PAB at 15 and 20 days from renneting.

Figure 6. Median values for initial CO_2 concentration measured in 9.5 weeks after renneting for old semi-hard Swiss-type cheese without PAB (a) and in 2 weeks after renneting for young semi-hard Swiss-type cheese with PAB (b). Horizontal and vertical error bars represent cheese position used and min and max values for assessed CO_2 respectively.

Figure 7. Experimental (red dots) and predicted (solid line) CO_2 concentration in the semi-hard cheese without PAB (a) and with PAB (b) CO_2 production after about 4 ripening days at 19°C. Root mean squared error (CVRMSD) is indicated on each figure. Error bars in experimental data represent standard deviations.

Figure 8. Predicted CO_2 gradients in cheese (solid lines) after 1, 2, 3, 4 and 10 days of contact with 100% CO_2, calculated considering 1.7 folds higher CO_2 production rate (19°C). Red

solid line and red error bars correspond to predicted and experimental CO_2 gradient after 4 days of contact.

Figure 9. Predicted CO_2 gradients in cheese (solid or dotted lines) after 1, 2, 3, 4 and 10 days of contact with 100% CO2, calculated considering 2 folds higher initial CO_2 gradient (19°C). Red solid line and red error bars correspond to predicted and experimental CO_2 gradient after 4 days of contact.

Figure 10. Effect of the intensity (low, medium and high, as stated in Table 2, in black, blue and red respectively) of the input parameter CO_2 solubility (a), diffusivity (b) permeability (c) and production rate (d) on the predicted CO_2 gradients in cheese ripened for 4 days at 19°C (age at beginning of ripening equalled 14 days from renneting).

Comment citer ce document :
Acerbi, F., Guillard, V., Saubanere, M., Guillaume, C., Gontard, N. (2018). Modelling CO 2 transfer in foil ripened semi-hard Swiss-type cheese. Journal of Food Engineering, 222, 73-83. ,
DOI : 10.1016/j.jfoodeng.2017.10.025

Table 1. Target chemical composition of “old” and “young” cheeses and steps of model validation

Type of cheese	Time after renneting	Target moisture % w/w	Target fat absolute % d.m.	Target salt content % NaCl/d.m.	Target pH	PAB	Validation step
“Old cheese”	15 days	42	40	5 %	5.45	No	❶ CO_2 diffusion only
“Young cheese”	9.5 weeks	42	8	2.5 %	5.45	Yes*	❷ CO_2 diffusion + production by PAB ❸ CO_2 diffusion + production by PAB + CO_2 permeation through ripening foil

*10^6 CFU ml^{-1} milk

Comment citer ce document :
Acerbi, F., Guillard, V., Saubanere, M., Guillaume, C., Gontard, N. (2018). Modelling CO 2 transfer in foil ripened semi-hard Swiss-type cheese. Journal of Food Engineering, 222, 73-83. ,
DOI : 10.1016/j.jfoodeng.2017.10.025

Table 2. Range of values used in the simulations

Parameter/level	low	medium	high
Solubility (mmol kg^{-1} atm^{-1})	25	36	40
Diffusivity (10^{-10} m^2s^{-1})	1	4	8
Permeability (cm^3 µm m^{-2} d^{-1} bar^{-1})	4000	44000	440 000
Production rate (mmol kg^{-1} d^{-1})	2	4	8

Comment citer ce document :
Acerbi, F., Guillard, V., Saubanere, M., Guillaume, C., Gontard, N. (2018). Modelling CO 2 transfer in foil ripened semi-hard Swiss-type cheese. Journal of Food Engineering, 222, 73-83. ,
DOI : 10.1016/j.jfoodeng.2017.10.025

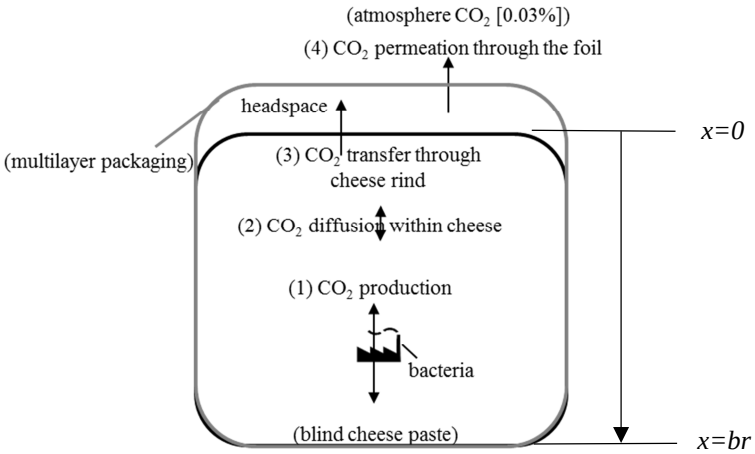

Figure 1: Scheme of the simplified food / packaging system with the four phenomena considered (mono-directional transfer through the headspace/cheese interface, *br* =cheese bottom-rind)

Comment citer ce document :
Acerbi, F., Guillard, V., Saubanere, M., Guillaume, C., Gontard, N. (2018). Modelling CO 2 transfer in foil ripened semi-hard Swiss-type cheese. Journal of Food Engineering, 222, 73-83. ,
DOI : 10.1016/j.jfoodeng.2017.10.025

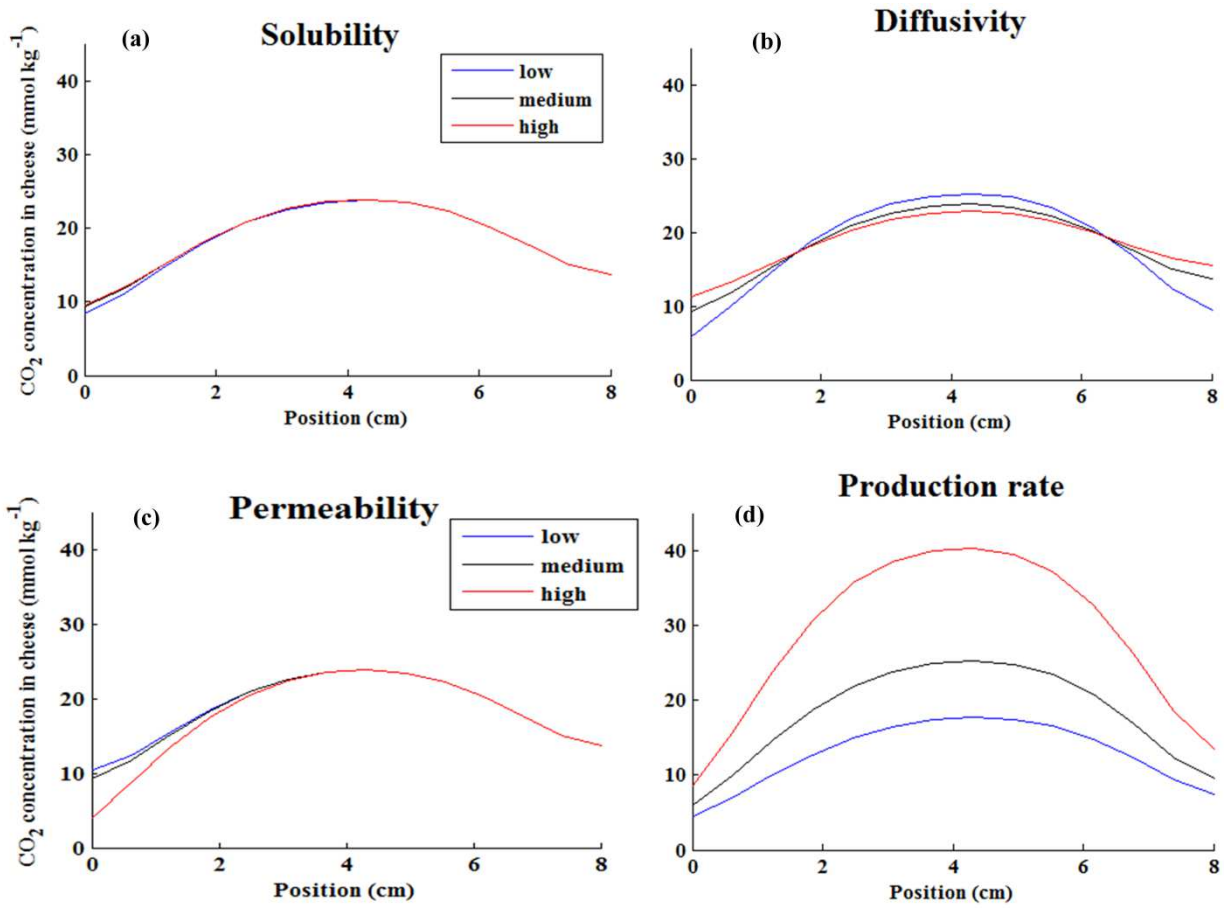

Figure 10. Effect of the intensity (low, medium and high, as stated in Table 2, in black, blue and red respectively) of the input parameter CO_2 solubility (a), diffusivity (b) permeability (c) and production rate (d) on the predicted CO_2 gradients in cheese ripened for 4 days at 19°C (age at beginning of ripening equalled 14 days from renneting).

Comment citer ce document :
Acerbi, F., Guillard, V., Saubanere, M., Guillaume, C., Gontard, N. (2018). Modelling CO 2 transfer in foil ripened semi-hard Swiss-type cheese. Journal of Food Engineering, 222, 73-83. ,
DOI : 10.1016/j.jfoodeng.2017.10.025

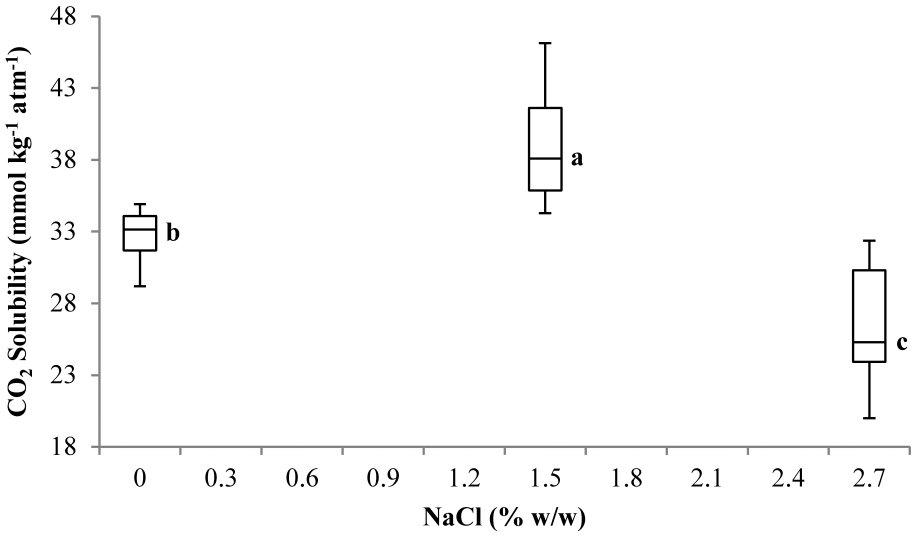

Figure 2. CO_2 solubility in semi-hard Swiss-type cheese as a function of salt content at 13°C. The point at intermediate NaCl content (1.5% w/w) is added to the ones reported by Acerbi et al. (2016b) and it was measured with same protocol on the same cheese. Different letters a, b c, …denote significant difference for $\alpha = 0.05$.

Comment citer ce document :
Acerbi, F., Guillard, V., Saubanere, M., Guillaume, C., Gontard, N. (2018). Modelling CO 2 transfer in foil ripened semi-hard Swiss-type cheese. Journal of Food Engineering, 222, 73-83. ,
DOI : 10.1016/j.jfoodeng.2017.10.025

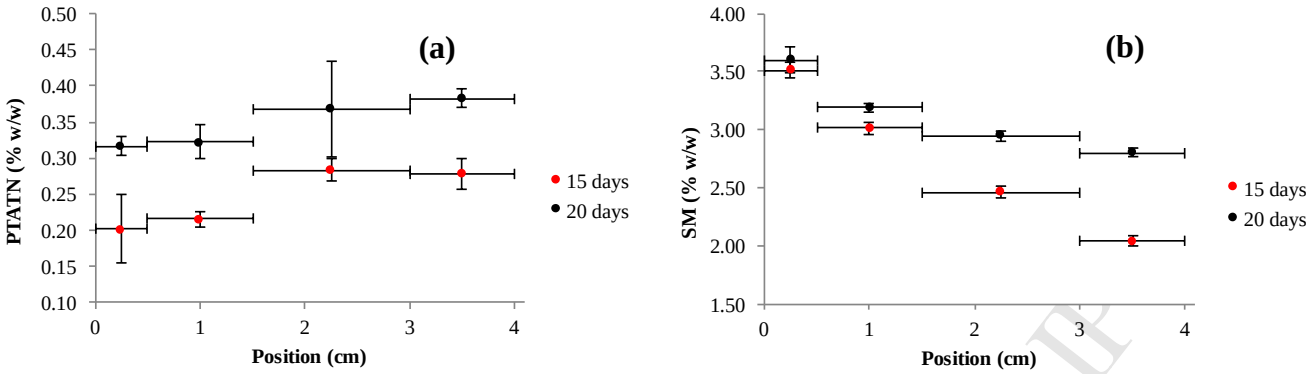

Figure 3. (a) PTATN - ratio of phosphotungstic acid soluble nitrogen on total nitrogen and (b) SM - salt in moisture ratio- in different positions of the of the semi-hard Swiss-type cheese with PAB, from rind (0 cm) to core (4 cm) at 15 and 20 days from renneting, representing starting time and ending time of the validation experiment.

Comment citer ce document :
Acerbi, F., Guillard, V., Saubanere, M., Guillaume, C., Gontard, N. (2018). Modelling CO 2 transfer in foil ripened semi-hard Swiss-type cheese. Journal of Food Engineering, 222, 73-83. ,
DOI : 10.1016/j.jfoodeng.2017.10.025

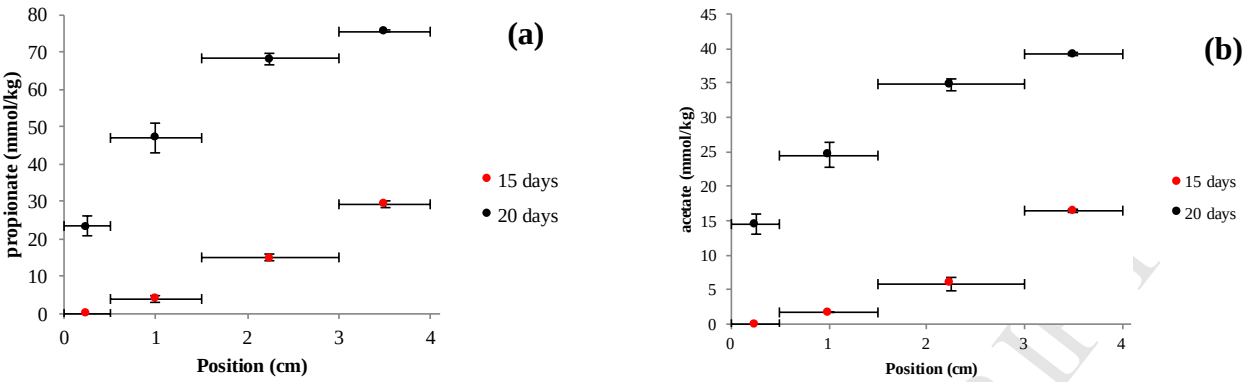

Figure 4. Propionate (a) and acetate (b) concentrations in different positions of the semi-hard Swiss-type cheese with PAB at 15 and 20 days from renneting (young cheese).

Comment citer ce document :
Acerbi, F., Guillard, V., Saubanere, M., Guillaume, C., Gontard, N. (2018). Modelling CO 2 transfer in foil ripened semi-hard Swiss-type cheese. Journal of Food Engineering, 222, 73-83. ,
DOI : 10.1016/j.jfoodeng.2017.10.025

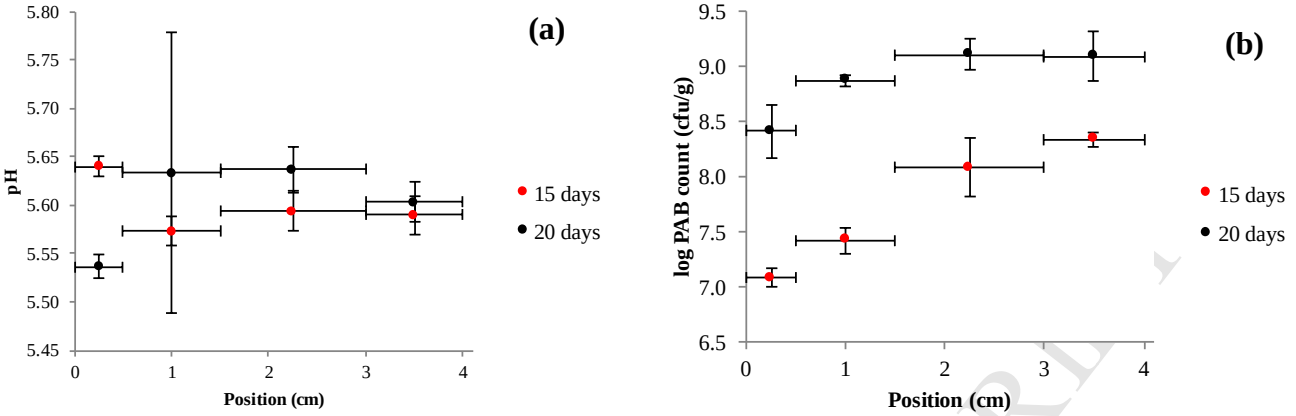

Figure 5. pH and PAB count in different positions of the semi-hard Swiss-type cheese with PAB at 15 and 20 days from renneting.

Comment citer ce document :
Acerbi, F., Guillard, V., Saubanere, M., Guillaume, C., Gontard, N. (2018). Modelling CO 2 transfer in foil ripened semi-hard Swiss-type cheese. Journal of Food Engineering, 222, 73-83. ,
DOI : 10.1016/j.jfoodeng.2017.10.025

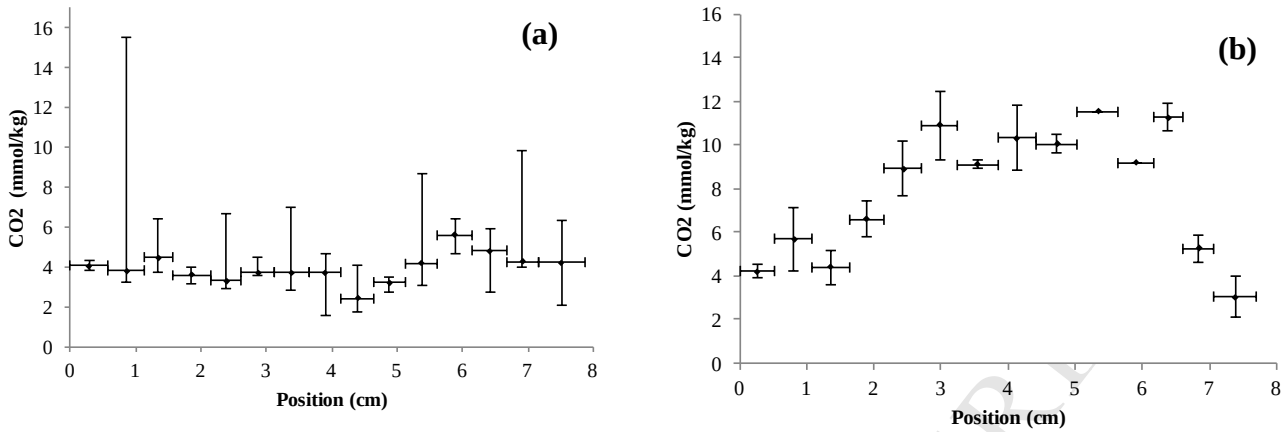

Figure 6. Median values for initial CO_2 concentration measured in 9.5 weeks after renneting for old semi-hard Swiss-type cheese without PAB (a) and in 2 weeks after renneting for young semi-hard Swiss-type cheese with PAB (b). Horizontal and vertical error bars represent cheese position used and min and max values for assessed CO_2 respectively.

Comment citer ce document :
Acerbi, F., Guillard, V., Saubanere, M., Guillaume, C., Gontard, N. (2018). Modelling CO 2 transfer in foil ripened semi-hard Swiss-type cheese. Journal of Food Engineering, 222, 73-83. ,
DOI : 10.1016/j.jfoodeng.2017.10.025

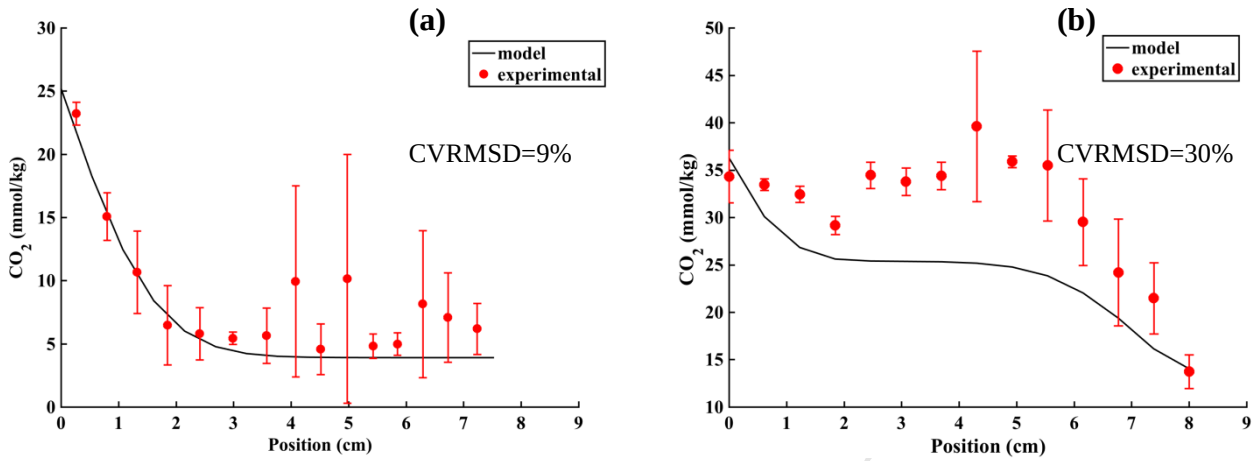

Figure 7. Experimental (red dots) and predicted (solid line) CO_2 concentration in the semi-hard cheese without PAB (a) and with PAB (b) CO_2 production after about 4 ripening days at 19°C. Root mean squared error (CVRMSD) is indicated on each figure. Error bars in experimental data represent standard deviations.

Comment citer ce document :
Acerbi, F., Guillard, V., Saubanere, M., Guillaume, C., Gontard, N. (2018). Modelling CO 2 transfer in foil ripened semi-hard Swiss-type cheese. Journal of Food Engineering, 222, 73-83. ,
DOI : 10.1016/j.jfoodeng.2017.10.025

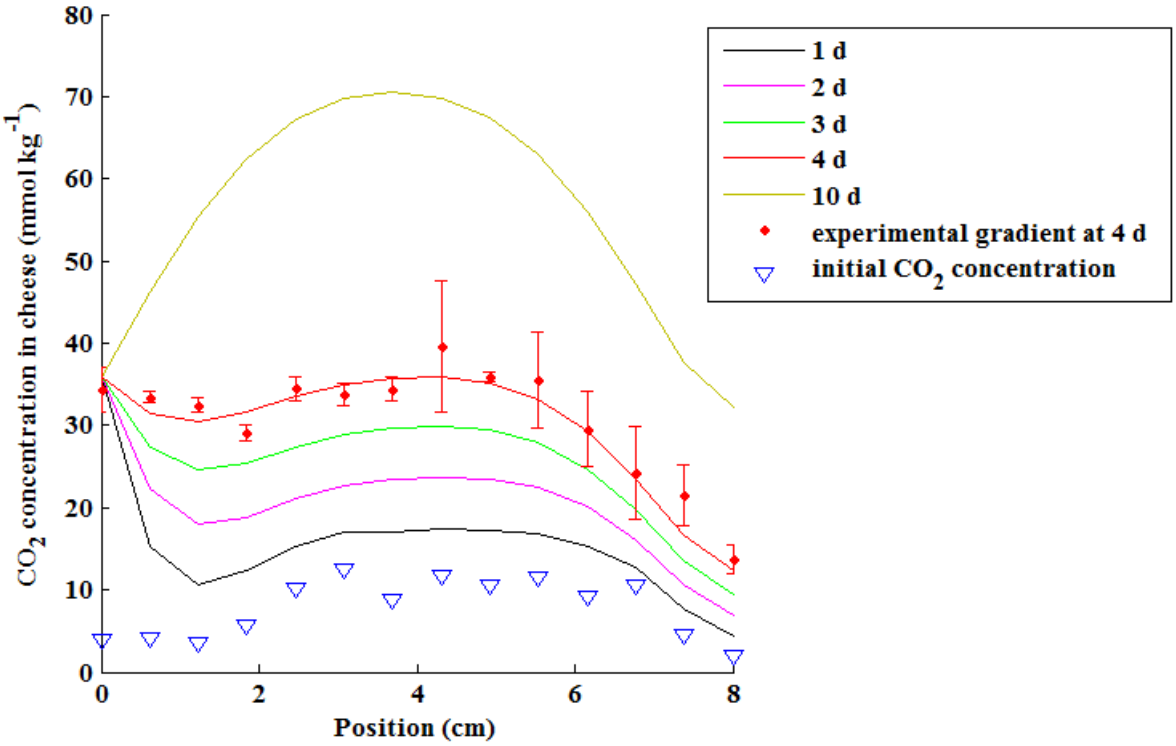

Figure 8. Predicted CO_2 gradients in cheese (solid lines) after 1, 2, 3, 4 and 10 days of contact with 100% CO_2, calculated considering 1.7 folds higher CO_2 production rate (19°C). Red solid line and red error bars correspond to predicted and experimental CO_2 gradient after 4 days of contact

Comment citer ce document :
Acerbi, F., Guillard, V., Saubanere, M., Guillaume, C., Gontard, N. (2018). Modelling CO 2 transfer in foil ripened semi-hard Swiss-type cheese. Journal of Food Engineering, 222, 73-83. ,
DOI : 10.1016/j.jfoodeng.2017.10.025

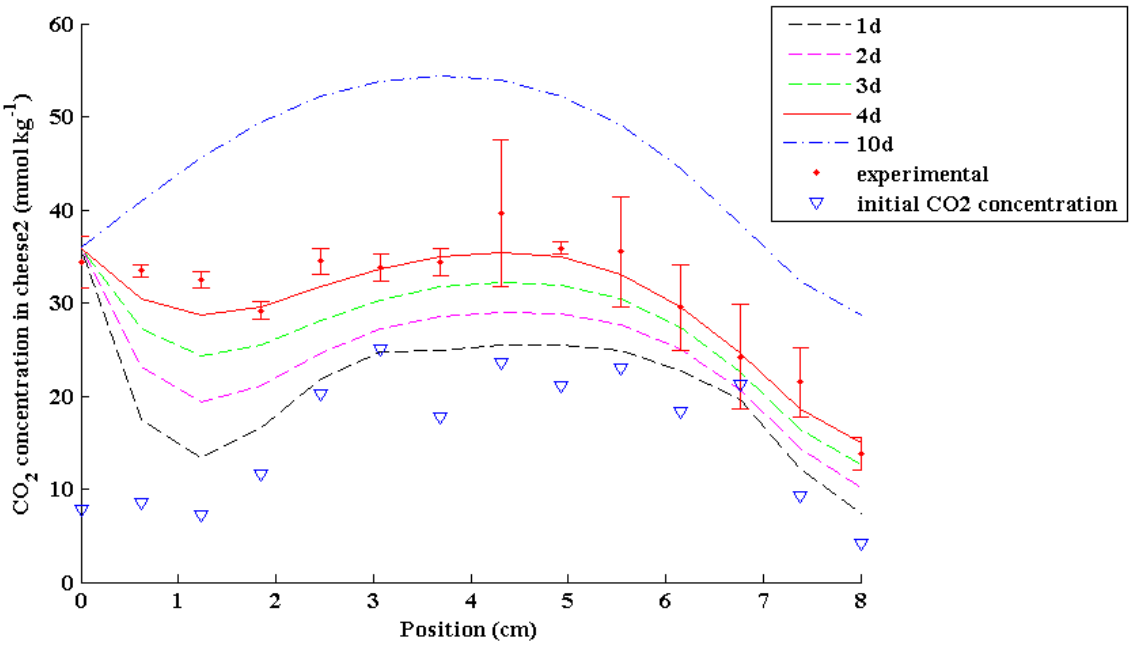

Figure 9. Predicted CO_2 gradients in cheese (solid or dotted lines) after 1, 2, 3, 4 and 10 days of contact with 100% CO2, calculated considering 2 folds higher initial CO_2 gradient (19°C). Red solid line and red error bars correspond to predicted and experimental CO_2 gradient after 4 days of contact.

Comment citer ce document :
Acerbi, F., Guillard, V., Saubanere, M., Guillaume, C., Gontard, N. (2018). Modelling CO 2 transfer in foil ripened semi-hard Swiss-type cheese. Journal of Food Engineering, 222, 73-83. ,
DOI : 10.1016/j.jfoodeng.2017.10.025

Highlights

- We proposed the first validated model for the prediction of CO_2 gradient in cheese.
- CO_2 production is the most important parameter affecting CO_2 gradients in cheese.
- A variation of a factor 10 of CO_2 permeability of the packaging did not relevantly affect CO_2 gradients in cheese
- ~~CO_2 permeability of the packaging did not relevantly affect CO_2 gradients in cheese.~~

Comment citer ce document :
Acerbi, F., Guillard, V., Saubanere, M., Guillaume, C., Gontard, N. (2018). Modelling CO 2 transfer in foil ripened semi-hard Swiss-type cheese. Journal of Food Engineering, 222, 73-83. ,
DOI : 10.1016/j.jfoodeng.2017.10.025